

This work is on a Creative Commons Attribution 4.0 International (CC BY 4.0) license, <https://creativecommons.org/licenses/by/4.0/>. Access to this work was provided by the University of Maryland, Baltimore County (UMBC) ScholarWorks@UMBC digital repository on the Maryland Shared Open Access (MD-SOAR) platform.

Please provide feedback

Please support the ScholarWorks@UMBC repository by emailing scholarworks-group@umbc.edu and telling us what having access to this work means to you and why it's important to you. Thank you.

Bolt loosening detection in a jointed beam using empirical mode decomposition-based nonlinear system identification method

International Journal of Distributed
Sensor Networks
2019, Vol. 15(9)
© The Author(s) 2019
DOI: 10.1177/1550147719875656
journals.sagepub.com/home/dsn


Chao Xu¹ , Chen-Chen Huang¹ and Wei-Dong Zhu² 

Abstract

In this work, a state-of-art nonlinear system identification method based on empirical mode decomposition is utilized and extended to detect bolt loosening in a jointed beam. This nonlinear system identification method is based on identifying the multi-scale dynamics of the underlying system. Only structural dynamic response signals are needed to construct a reduced-order model to represent the system concerned. It makes the method easy to use in practice. A new bolt loosening identification procedure based on the constructed system nonlinear reduced-order model is proposed. A new damage feature to indicate bolt loosening is presented. Experimental works are carried out to validate the proposed method. The results show that the proposed damage detection method can detect bolt loosening effectively, and the proposed damage feature values increase with the increase of bolt torques. The damage feature calculated from the response solution of the reduced-order model can give robust and sensitive indication of bolt loosening.

Keywords

Bolt loosening, nonlinear system identification, reduced-order model, empirical mode decomposition, damage diagnosis

Date received: 13 June 2019; accepted: 14 August 2019

Handling Editor: Edward Bednarz

Introduction

Bolted joints are widely used in various structures and machines. Significant advantages of using bolted joints are that they can be easily disassembled and the possibility to design for bearing a large tension load. During the whole service period, bolted joints may be subjected to a variety of failure modes such as self-loosening, slip-page, shaking apart, fatigue cracks, and so on. Among them, self-loosening is the most common issue, especially as jointed structures are under vibration excitations.¹ Therefore, identifying loosening in a bolted joint plays an important role not only to prevent failures but also to ensure appropriate functioning of engineering structures.

Structural health monitoring (SHM) is generally referred to the process of implementing a method of

structural identification and damage detection.^{2,3} Many SHM techniques are based on a simple, yet effective, principle that structural dynamic properties change in the presence of certain defects in a structure. Generally, there are two main categories of current SHM techniques: local and global approaches. A number of local SHM techniques have been developed to assess local bolt loosening in a jointed structure. For example, the

¹School of Astronautics, Northwestern Polytechnical University, Xi'an, China

²Department of Mechanical Engineering, University of Maryland Baltimore County, Baltimore, MD, USA

Corresponding author:

Chao Xu, School of Astronautics, Northwestern Polytechnical University, Xi'an 710072, China.

Email: chao_xu@nwpu.edu.cn



Creative Commons CC BY: This article is distributed under the terms of the Creative Commons Attribution 4.0 License (<http://www.creativecommons.org/licenses/by/4.0/>) which permits any use, reproduction and distribution of the work

without further permission provided the original work is attributed as specified on the SAGE and Open Access pages (<https://us.sagepub.com/en-us/nam/open-access-at-sage>).

methods based on ultrasonic elastic wave propagation,⁴⁻⁶ time reversal technique,^{7,8} acousto-elastic technique,⁹ and electromechanical impedance^{10,11} are extensively studied. However, most of the local SHM approaches rely on point sensors, or sensors that obtain data on a local small area. Thus, numerous sensors and cables are required for applying them in a complicated assembled structure where thousands of bolts are included.

Compared to local SHM approaches, the SHM techniques based on vibration analysis can be thought as global SHM approaches. The most popular vibration features used in a vibration-based SHM method are system modal properties, such as normal mode frequencies, mode shapes, and modal damping ratios.¹² However, Todd et al.¹³ carried out theoretical and experimental studies and found that those global modal properties were relatively insensitive for effectively detecting changes in bolt preload. Then, they proposed a novel vibration-based SHM technique based on using nonlinear chaotic excitation and nonlinear dynamics theory to detect joint degradation, and an improvement in preload loss detectability was experimentally validated.¹⁴ But, both an unusual chaotic excitation and a complex nonlinear dynamics analysis method are needed, which make the method not easily implemented in practice. Caccese et al.¹⁵ proposed a method based on the vibration transfer function derived as the complex ratio between Fourier transform of a response point signal and Fourier transform of a reference point signal for identifying bolt loosening in a hybrid composite/metal bolted joint. It is concluded that the proposed transfer function method had much promise for detecting bolt loosening over the modal analysis method. Milanese et al.¹⁶ presented a method to detect joint loosening using output-only broadband vibration data. A time-domain vibration feature based on basic statistical properties of the measured strains and their time derivatives, and a frequency domain vibration feature based on the signal power in different frequency bands were proposed. Recently, Huda et al.¹⁷ used non-contact laser excitation vibration tests to detect bolt loosening, where the resulted structural high frequency response signals were analyzed to extract loosening features. Esmaeel and Taheri¹⁸ presented a method to detect bolt loosening in single lap joint, where the method of the empirical mode decomposition (EMD) was used to analyze measured vibration response signals, and a signal energy-based damage index (DI) was proposed. However, it is noted that all the above works use only the linear vibration information of the concerned structure.

It is well known that the discontinuity due to joint interface introduces nonlinear stiffness and damping to an assembled structure.¹⁹ From the view of structural dynamics, the problem of identifying bolt loosening in

a jointed structure can be solved in the frame of nonlinear system identification (NSI).²⁰ Crawley and Aubert²¹ proposed a force-state mapping method for identification of nonlinear joint elements. Ma et al.²² presented a nonlinear identification method for bolted joints by using the difference in the dynamics between the bolted structure and a monolithic structure without bolted joints. A bolt loosening detection method based on identification of structural sub-harmonic resonance was proposed by Zhang et al.²³ Roettgen and Allen²⁴ studied nonlinear characterization of a bolt-jointed structure by using a nonlinear normal modal framework.

In a recent work, a state-of-art NSI method based on relating the analytical and empirical slow-flow dynamics using EMD²⁵ has been proposed.^{26,27} EMD is a very powerful time-frequency analysis technique and suitable for analyzing nonlinear and nonstationary signals. By using EMD to measured response signals, an empirical slow-flow dynamics model can be obtained, which is in correspondence with an analytical slow-flow model.²⁸ Then, a nonlinear interaction model (NIM) consisting of a set of intrinsic modal oscillators (IMOs) to characterize system local dynamics can be determined. The NIM can be viewed as a nonlinear reduced model of the underlying structural system. This EMD-based NSI has been used to study dynamics of some typical nonlinear systems.^{29,30} Especially, utilizing the method to identify nonlinear dynamics of a vibro-impact beam has been carried out numerically in Kurt et al.³¹ and experimentally in Chen et al.³² Very recently, Sadeghi and Lotfan³³ used this EMD-based NSI method to identify nonlinear parameters of a cantilever beam supported with a cubic stiffness spring at the free end.

To date, the state-of-art EMD-based NSI method has shown much promise to model complicated nonlinear structures, but damage identification based on this method has not been paid much attention, especially for bolt loosening identification. In this article, the NSI method based on EMD is utilized and extended to identify bolt loosening in a jointed beam. The aim is to provide a new approach for identifying bolt loosening in a structure based on the constructed system nonlinear reduced-order model. The article is organized as follows. A brief introduction to the EMD-based NSI method is given in "EMD-based NSI method" section. The proposed bolt loosening identification method based on the EMD-based NSI method is given in "Loosening identification based on constructed system reduced-order model" section. A bolt loosening detection experiment to validate the proposed method is described in "Experimental study" section. The detection results and related discussion are given in "Results and Discussion" section. Conclusions are given in "Conclusions" section.

EMD-based NSI method

The EMD method is a very powerful tool for analyzing nonlinear and nonstationary time series signals. In contrast to the classic Fourier transform and wavelet transform, the EMD decomposes given data into intrinsic mode functions (IMFs) that are not set analytically and are instead determined by an analyzed sequence alone.³⁴ Generally, an IMF represents a hidden oscillation mode that is embedded in the time signal such that each IMF represents its own characteristic time scale and the original time signal can be reconstructed by the linear superposition of the IMFs.³⁵ By performing the EMD method, a given signal $x(t)$ can be decomposed as follows

$$x(t) = \sum_{j=1}^n c_j(t) + r_{n+1}(t) \quad (1)$$

where $c_j(t)$ is the j th IMF and $r_{n+1}(t)$ represents the residue of the data $x(t)$ after n numbers of IMFs are extracted.

The procedure of the EMD decomposition can be categorized into the following steps.

- Determine all the local maxima and minima from the given signal $x(t)$.
- Compute the upper and lower envelopes, $e_{\max}(t)$ and $e_{\min}(t)$, by spline interpolating the minima and maxima of the signal.
- Designate their mean $R(t) = (e_{\max}(t) + e_{\min}(t))/2$.
- Extract the remainder signal $c(t) = x(t) - R(t)$.
- The remainder signal $c(t)$ is analyzed by the same above four steps as if it was new data until the residual mean value $R(t)$ is smaller than a prescribed tolerance. Once the criterion is satisfied, the final remainder signal $c_1(t)$ is regarded as the first IMF of the given signal $x(t)$.

Generally, the first IMF contains a component which has the finest scale and possesses the highest frequency. By removing c_1 from the original signal $x(t)$, and repeating the above algorithm iteratively to the new remainder signal, additional IMFs can be extracted.

It is well known that the standard EMD method has two disadvantages: one is called end effect, and another is the problem of mode mixing. End effect is the observation that the numerical artifacts in decomposition become prominent near the beginning and the end of the signal, because the spline interpolation through the extrema becomes prominent near the initial and the final period. Mode mixing is defined as a single IMF such as oscillations of dramatically disparate scales or a component of a similar scale residing in different IMFs. To overcome the above two drawbacks, the techniques

of mirror-image signal and masking signal can be used. By including these methods to the algorithm of the standard EMD, an advanced EMD (AEMD) method is proposed in Lee et al.²⁸

The aim of employing a mirror-image signal is to expand the time series, so that the end effect does not occur to the original time series. Denote the original time series by $x(t)$, $t \in [0, t_f]$, and then the mirror-image signal is defined by $x_{\text{mir}}(t)$, $t \in [-t_f, 0)$

$$x_{\text{mir}}(t) = \begin{cases} x(-t), & \text{for } |\dot{x}(t)|_{t=0^+} < \epsilon \\ -x(-t), & \text{otherwise} \end{cases} \quad (2)$$

where ϵ is a small positive number. By adding the mirror-image signal at the original signal's start point, the original time series is expanded. Thus, the new expanded signal is defined by $x_{\text{expand}}(t) = \{x_{\text{mir}}(t); x(t)\}^T$, $t \in [-t_f, t_f]$. With the mirror-image signal, the end effect in the initial period of the time series could be erased. For the end effect in the final period of the time series, we could also apply the mirror-image signal in a similar way.

The aim of employing a masking signal is to alleviate the problem of mode mixing. The masking signal is usually a harmonic with its frequency equal to the highest frequency (this can be obtained with a spectral analysis) in the original time series. Turning a masking signal to the highest-frequency component can yield clear separation of the highest-frequency components, in particular, as it is weak and buried compared with the other harmonics. When the highest-frequency component was separated as the highest-frequency IMF, the residual could still employ the masking signal. Sequentially, the lower components can also yield clear separation.

By performing EMD on the measured time signal, a complete and nearly orthogonal basis of IMFs at each sensing location can be yielded. Therefore, EMD provides a multi-scale decomposition of a measured time signal into embedded oscillatory modes at different time scales of the dynamics.³² Recently, the physics-based foundation for EMD has been provided by Lee et al.²⁸ It has been shown that performing slow/fast partition of the extracted IMFs results in a set of slowly varying amplitude that are nearly identical to the response of the underlying analytical slow-flow mode. Therefore, by utilizing EMD, a reduced-order empirical slow-flow model of the dynamics can be obtained. The principle of the correspondence between analytical and empirical slow-flows is briefly summarized here.

Considering an n -degree-of-freedom (DOF) dynamical system, it may be defined as follows

$$\dot{X} = f(X, t), X = \{x, \dot{x}\}^T \in \mathbb{R}^{2n}, t \in \mathbb{R} \quad (3)$$

where x and \dot{x} represent the displacement and velocity vectors of the system, respectively; f is the system function, which is often unknown during the system identification procedure. It is assumed that the dynamic response of the system contains N distinct, nearly harmonic components at frequencies $\omega_1 > \dots > \omega_N$, and the response of the k th DOF can be expressed as a summation of N independent components, defined as follows

$$x_k(t) = x_k^1(t) + x_k^2(t) \dots + x_k^N(t), k = 1, 2 \dots N \quad (4)$$

where $x_k^m(t)$ indicates m th harmonic component corresponding to the frequency ω_m . For each component $x_k^m(t)$, a new complex variable can be defined

$$\begin{aligned} \psi_k^m(t) &= \dot{x}_k^m(t) + j\omega_m x_k^m(t) = \varphi_k^m(t) e^{j\omega_m t}, \\ j &= \sqrt{-1}, m = 1, \dots, N \end{aligned} \quad (5)$$

where $\psi_k^m(t)$ represents the complex slow partition of the dynamics, $e^{j\omega_m t}$ represents the fast partition of the dynamics. Substituting equations (4) and (5) into equation (3) and by employing the complexification-averaging (CX-A) technique to eliminate the fast dynamics partition,²⁴ the analytical slow-flow of equation (3) can be obtained

$$\dot{\varphi}_k = F(\varphi_1, \dots, \varphi_n), \varphi_k \in C^N \quad (6)$$

where $\varphi_k = \{\varphi_k^1, \dots, \varphi_k^N\}$. It can be found that the dimensionality of the slow-flow is determined by the number of fast frequencies and the slow-flow model represents the slow evolution of the N harmonic components.

Comparing equations (1) and (4), it can be found that the response signal is expressed in a similar way. To build the equivalence between the analytical slow-flow and EMD, Lee et al.²⁸ defined a complex function with Hilbert transform (HT) to complexity the m th IMF $c_k^m(t)$ extracted from EMD, that is

$$\hat{\psi}_k^m(t) = c_k^m(t) + j\mathcal{H}[c_k^m(t)] = \hat{A}_k^m(t) e^{j\hat{\theta}_m^k(t)} \quad (7)$$

where $\mathcal{H}[\cdot]$ denotes HT, $\hat{A}_k^m(t)$ and $\hat{\theta}_m^k(t)$ are the instantaneous amplitude and phase of the m th IMF, respectively, and they can be compute by

$$\hat{A}_k^m(t) = \sqrt{[c_k^m(t)]^2 + \mathcal{H}[c_k^m(t)]^2}, \hat{\theta}_m^k(t) = \tan^{-1} \left\{ \frac{\mathcal{H}[c_k^m(t)]}{c_k^m(t)} \right\} \quad (8)$$

Equation (7) is in a form similar to the slow-flow analysis equation (5). Thus, equation (7) can also be written as a slow-fast representation

$$\hat{\psi}_k^m(t) = \hat{A}_k^m(t) e^{j\hat{\theta}_m^k(t) - j\omega_m t} e^{j\omega_m t} \quad (9)$$

in which, $\hat{A}_k^m(t) e^{j\hat{\theta}_m^k(t) - j\omega_m t}$ is the slow component and $e^{j\omega_m t}$ is the fast component. When multiplied by $j\omega_m$, this analytical function appears identical to the complex variable in equation (5) under the condition that the m th IMF is associated with the m th harmonic component.

Finally, the correspondence between the analytical slow dynamics and the empirical slow dynamics of the k th DOF of the system can be obtained³⁵

$$\underbrace{\varphi_k^m(t)}_{\text{Analytical slow dynamics}} = \underbrace{j\omega_m \hat{A}_k^m(t) e^{j\hat{\theta}_m^k(t) - j\omega_m t}}_{\text{Empirical slow dynamics}} \quad (10)$$

where $\hat{A}_k^m(t)$ and $\hat{\theta}_m^k(t)$ can be obtained through equation (8).

Based on the equivalence between the analytical slow dynamics and the empirical slow dynamics, a reduced-order model can be constructed. The reduced-order model consists of sets of IMOs. Lee et al.²⁸ defined IMOs as the equivalent linear damped oscillators that can reproduce a measured time signal over different time scales. Each IMO can rebuild the response of the system associated with the dominant frequency of ω_m . It is assumed each IMO is a linear forced oscillator with viscous damping term. Its dynamics model corresponding to the m th component of the k th DOF of the system can be expressed as

$$\ddot{x}_k^m(t) + 2\xi_k^m \omega_m \dot{x}_k^m(t) + \omega_m^2 x_k^m(t) = F_k^m(t) \quad (11)$$

where ξ_k^m is the damping factor and ω_m is considered to be equal to the fast frequency of the m th IMF. The forcing function, $F_k^m(t)$, represents the interaction of the m th component with the other components of the k th DOF. It is expressed as

$$\begin{aligned} F_k^m(t) &= \text{Re}[\Lambda_k^1(t) e^{j\omega_1 t} + \Lambda_k^2(t) e^{j\omega_2 t} + \dots + \Lambda_k^m(t) e^{j\omega_m t} \\ &\quad + \dots + \Lambda_k^N(t) e^{j\omega_N t}] \end{aligned} \quad (12)$$

where $\text{Re}[\cdot]$ represents the real part. However, IMO is a linear oscillator; thus, in all components of the $F_k^m(t)$, only the component with fast frequency ω_m can produce the dynamic response with frequency ω_m . Thus, the $F_k^m(t)$ can be simplified as

$$F_k^m(t) = \text{Re}[\Lambda_k^m(t) e^{j\omega_m t}] \quad (13)$$

in which $\Lambda_k^m(t)$ represents the slowly varying forcing amplitude. The forcing amplitudes are obtained as³⁵

$$\begin{aligned} \Lambda_k^m(t) &\approx 2[\dot{\varphi}_k^m(t) + \xi_k^m \omega_m \varphi_k^m(t)] \\ &\approx 2 \left[\frac{d}{dt} \left(j\omega_m \hat{A}_m(t) e^{j[\hat{\theta}_m(t) - \omega_m t]} \right) + j\xi_k^m \omega_m^2 \hat{A}_m(t) e^{j[\hat{\theta}_m(t) - \omega_m t]} \right] \end{aligned} \quad (14)$$

where $\hat{A}_m(t)$ and $\hat{\theta}_m(t)$ can be computed by equation (8), ω_m is directly determined by performing Fast Fourier analysis of the measured time series. The viscous damping ratio ξ_k^m is selected by minimizing the normalized mean square errors between the envelope of the IMF and the IMO solution. Thus, $F_k^m(t)$ can be determined and the identified IMO can reproduce the m th IMF with an expected accuracy.

In practice, the analytical model of the system concerned is unknown. However, based on the previous discussion, an NSI method can be developed based on the EMD of the measured time signals. The basic assumption is that the measured dynamics can be decomposed in terms of slowly modulated fast oscillations. The core of the NSI method is to build a reduced-order dynamics model of the system from measured time signals. The main procedure of the NSI method is summarized as follows.

First, for the system concerned, time series signals from multiple sensors throughout the system are measured. Impact hammer testing widely used in conventional experimental mode analysis can be used to excite the system. Then, IMFs at each sensing location can be extracted by applying EMD to the measured time signals. In this step, to improve EMD results, the techniques of mirror-image signal and masking signal are used. Based on the spectral analysis of the measured signals, the dominant IMFs can be identified and kept for further use. Thus, the basic time scale and the dimensionality of the dynamics can be determined. Next, relate the slow components of the dominant IMFs to the underlying slow-flow dynamics of the system. Based on the equivalence between the analytical slow dynamics and the empirical slow dynamics, sets of IMOs can be defined and identified, that is, a parametric reduced-order slow-flow model can be obtained. In next section, this state-of-art NSI method is extended to carry out quantitative detection of bolt loosening in jointed structures.

Loosening identification based on constructed system reduced-order model

It is well known that if certain defects occur to a structure, the dynamics of the structure will change. This is the basic concept of SHM. Similarly, in this article, it is natural to consider that if the structure changes, the constructed system reduced-order model using the NSI method in “EMD-based NSI model” section also changes. This is the basic idea of developing a new bolt loosening identification method based on the constructed reduced-order model. In another word, it is assumed that there exists difference between the identified IMOs for a healthy structure and for a damaged structure.

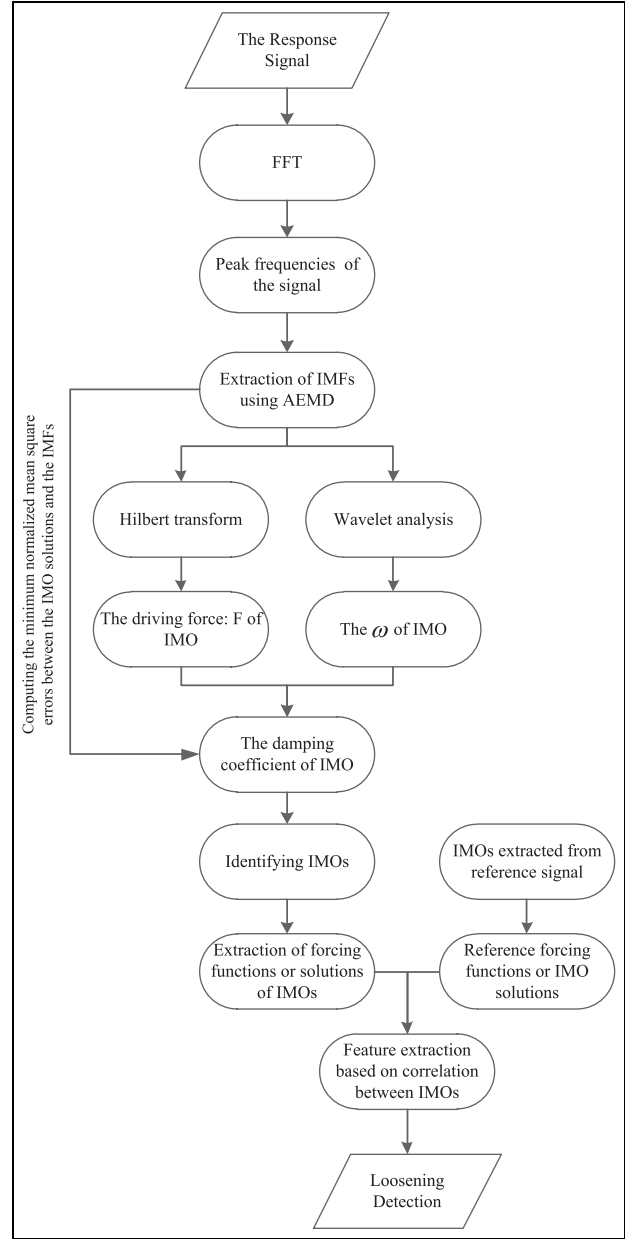


Figure 1. Outline of the proposed loosening identification method.

In this article, a new method to identify bolt loosening through the constructed IMOs is proposed. Different bolt torques may lead to different nonlinear dynamics of the structure, and different dynamics can lead to different IMOs. Recently, boundary impact identification utilizing the NSI method has been proposed by Kurt et al.³¹ and Chen et al.³² In their study, the Pearson’s linear correlation coefficient was computed for the slowly varying complex forcing amplitudes of all IMOs for a linear and a vibro-impact beam to indicate impact event. A dense array of acceleration sensors was required in their work to identify the

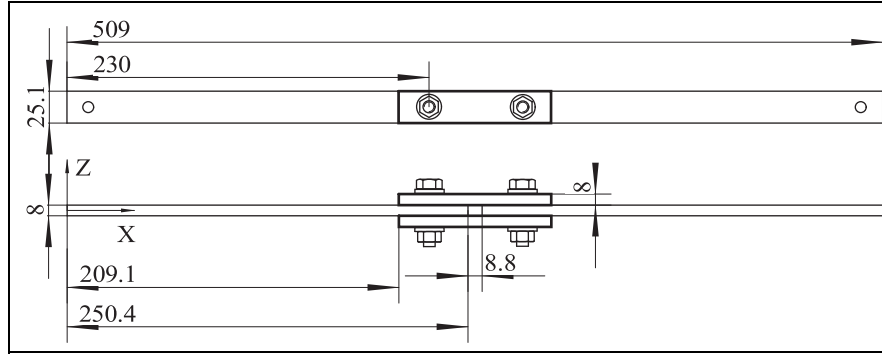


Figure 2. Bolted beam used in the experimental test (all dimensions given in mm).

impact location and instant. To overcome the limit, as a utilization and development of the EMD-based NSI method, a simple, yet effective, bolt loosening detection method is developed herein. For this proposed method, only fewer sensors are required for a joint and only the output response is used. Based on this sensor configuration, a loosening identification method is given as shown in Figure 1.

First, the structural response, which can be acceleration, velocity, or displacement, is measured. The measured signal is first noise-filtered and then the enhanced AEMD method, which includes employing the techniques of mirror-image signal and masking signal, is carried out to extract IMFs. With obtained IMFs, we employ slow-flow analysis and HT, a set of IMOs could be established. The IMOs are in the form as follows

$$\ddot{x}_k^m(t) + 2\xi_k^m \omega_m \dot{x}_k^m(t) + \omega_m^2 x_k^m(t) = F_k^m(t), m = 1, 2 \dots N \quad (15)$$

where k denotes the sensor location, m denotes the m th IMO of the dynamics, ξ_k^m and ω_m are time-invariant coefficients, and the $F_k^m(t)$ is a time-varying forcing function. For each set of the IMOs corresponding to the dynamics obtained from the sensor, we can re-write these model parameters in a matrix as follows

$$\begin{bmatrix} \xi_k^1 & \omega_1 & F_k^1(t) \\ \xi_k^2 & \omega_2 & F_k^2(t) \\ \vdots & \vdots & \vdots \\ \xi_k^N & \omega_N & F_k^N(t) \end{bmatrix} \quad (16)$$

Then, it is assumed that bolt loosening may change the local dynamics and cause the change of the coefficients of IMOs. In this article, a loosening DI is defined to measure the difference between the healthy condition and the damaged condition. The time-varying variable u is used to represent the variables given by IMOs. The over-line symbol “ \sim ” is used to distinguish whether the variable is in the healthy condition or in the damaged condition. Thus, the loosening DI is defined by

$$DI = COR(u_i(t), \tilde{u}_i(t)) = \frac{\left[\sum_{i=1}^N |u_i^T \tilde{u}_i| \right]^2}{\left(\sum_{i=1}^N u_i^T u_i \right) \left(\sum_{i=1}^N \tilde{u}_i^T \tilde{u}_i \right)} \quad (17)$$

where i denotes the order of IMOs, \tilde{u}_i and u_i are time-varying variables given by IMOs for the healthy structure and the damaged structure, respectively. It is noted that the time-varying variable u_i can be the forcing term of an IMO, $F_k^m(t)$, or the dynamic solution of the IMO, $x_k^m(t)$. Kurt et al.³² used the time-varying forcing amplitude $F_k^m(t)$ to calculate the linear correlation coefficient in their work. However, it is found in this article that using the dynamic solution of the IMO instead can give more sensitive DI. It is noted that the proposed damage feature is much like the correlation coefficient in statistics analysis. The value of the proposed DI is between 0 and 1. The lower value of damage feature indicates the loosening state is more serious compared to the healthy state.

Experimental study

Experimental works are carried out to validate the proposed loosening detection method. A jointed beam with a central lap joint is considered as shown in Figure 2. The jointed beam is composed of two half-beams, and each half-beam is of length 509 mm, width 25.1 mm, and thickness 8 mm. They are joined by a double shear lap joint at its center. The beam is made of low-carbon steel with the density $\rho = 7800 \text{ kg/m}^3$ and Young's modulus $E = 200 \text{ GPa}$. Two grade 8.8 M8 steel bolts are used for installment. To reduce the effect of additional boundary conditions, the beam is suspended by a rubber cord at each end to simulate free-free boundary condition, as shown in Figure 3. The standard torque for the grade 8.8 M8 steel bolt is 24 Nm. Therefore, the bolts are torqued to 24 Nm by a digital torque wrench. This condition of bolt torque is considered as the healthy state.

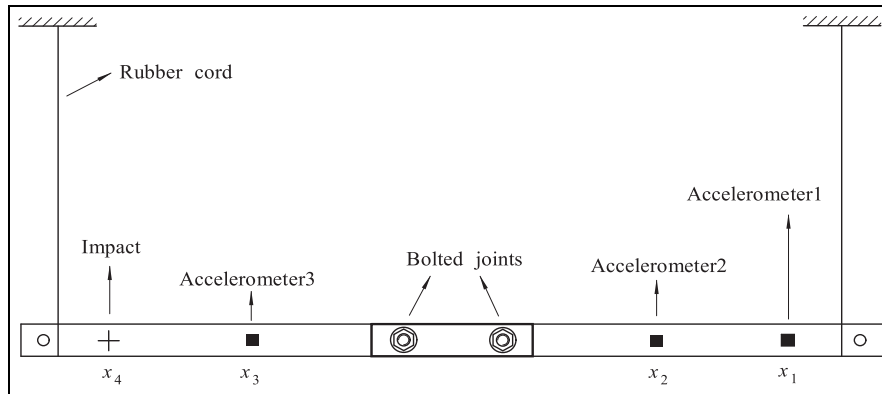


Figure 3. Experimental setup and the positions of the accelerometers and impulsive excitation.

A PCB Model 086C03 impact hammer with a hard metal tip is used to excite the beam. Input excitation forces were measured by the inner force transducer of the hammer. It is noted that the impact position should be chosen to avoid “near the node locations” of the first five mode shapes, which could be obtained by assuming the beam vibrate linearly. Acceleration sensors are used to measure structural response under the impact excitation. The type of acceleration sensor is PCB Model 333B32. It is noted that all input forces and output accelerations are applied and measured along the direction of z -axis. As shown in Figure 3, to study the effect of accelerometer measurement positions on detection effectiveness, three accelerometers are attached through wax-cement to the beam at different position: x_1 , x_2 and x_3 . The position x_4 is the impulsive excitation position. All of the points x_1 , x_2 , x_3 , and x_4 are on the longitudinal axis of symmetry of the beams.

To validate that the proposed method can detect bolt loosening quantitatively, we consider totally 12 different bolt torque values, which correspond to the torque value: 24, 22, 20, 18, 16, 14, 12, 10, 8, 6, 4, and 2 Nm. The aim is to validate whether the proposed method can identify the levels of bolt torque with a good resolution. To validate the repeatability and robustness of the proposed method, at each torque level, six assemble–disassemble–repeat tests are performed. Thus, totally 72 tests are carried out. At each test, three time-domain response signals from three accelerometers are measured.

Results and discussion

Results of NSI

An example of impact force input and recorded acceleration signals at the healthy state (under the standard bolt torque) is presented in Figure 4. It can be found that under the impulsive force excitation given by the hammer, structural acceleration response amplitudes

decay very fast due to joint interface damping. This phenomenon is accordance with other dynamic experimental results on jointed structure.^{19,36}

Then, the fast Fourier transform is conducted to find the main response peak frequencies. An example of the results of fast Fourier transform of acceleration response is shown in Figure 5. It can be found that the dominant frequency component can be up to about 3000 Hz. To consider the frequency bandwidth, the hammer can excite and reduce the measurement noise effect, a low-pass filter with the cutoff frequency of 3000 Hz is applied to the recorded raw signals. The EMD process is then carried out to these filtered signals.

In Figures 6–8, the IMFs extracted by applying EMD method for three acceleration time series recorded at the position x_1 , x_2 , and x_3 are shown, respectively. The corresponding time-frequency plots of the IMFs are also given. For the time-frequency analysis, the continuous wavelet transform method is applied. Specifically, a complex Morlet wavelet function named *cmor3-3* in MATLAB environment is implemented and the scale is set to 256. From these figures, it can be found five IMFs are extracted by using the enhanced AEMD method for each acceleration signal. The instantaneous frequency of the first IMF is about 2600 Hz and the fifth IMF is about 170 Hz. It can be found that the IMFs with high instantaneous frequency decay faster than the IMFs with lower frequency. The detailed analysis of the EMD results for a jointed beam was carried out and important information from EMD analysis by comparing with the EMD result for a monolithic beam was already given in Chao and Dong.³⁷ Each identified IMF almost can be considered as a mono-component signal and can be used by the NSI method introduced in “EMD-based NSI method” section.

By using the construction method for IMOs, an IMO can be obtained for each IMF. Thus, five IMOs

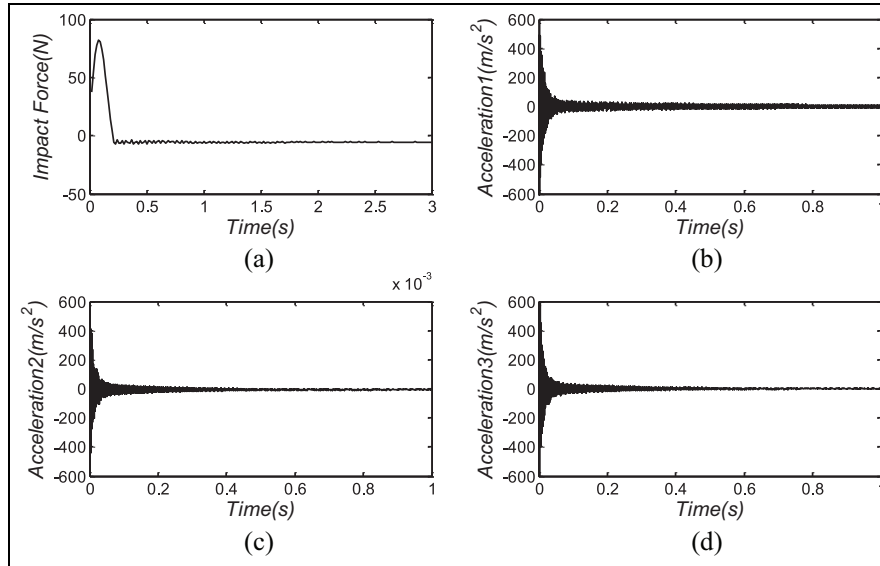


Figure 4. (a) Impact force, (b) acceleration signal at position x_1 , (c) acceleration signal at position x_2 , (d) acceleration signal at position x_3 .

are obtained. For example, by using the IMFs extracted from the acceleration signal recorded at the position x_1 , the following set of IMO model parameters can be obtained

$$\begin{bmatrix} 0.39 & 1080.5 & F_1(t) \\ 0.14 & 2630.4 & F_2(t) \\ 0.162 & 5007.6 & F_3(t) \\ 0.256 & 7816.4 & F_4(t) \\ 0.0385 & 11979 & F_5(t) \end{bmatrix}$$

The elements in the first column of this matrix are viscous damping ratios and in the second column are angular frequencies. The identified time-varying force functions are shown in Figure 9. To validate the accuracy of identified IMOs, we compute the numerical solutions of each IMO and compare them with the corresponding IMFs. As an example, in Figure 10, the comparisons between the second IMF with the corresponding IMO solutions at position x_1 , x_2 , and x_3 , are given. It can be found they agree well with each other. This validates the effectiveness of the constructed reduced model.

Results of bolt loosening identification

As mentioned previously, 72 measurements for 12 different bolt torque levels are recorded, each measurement has three response time series, that is, three acceleration time series recorded at three different positions: x_1 , x_2 , and x_3 . For each acceleration time series, we can employ EMD method to decompose the acceleration time series into a set of IMFs. For each IMF, we establish an IMO which can approximately

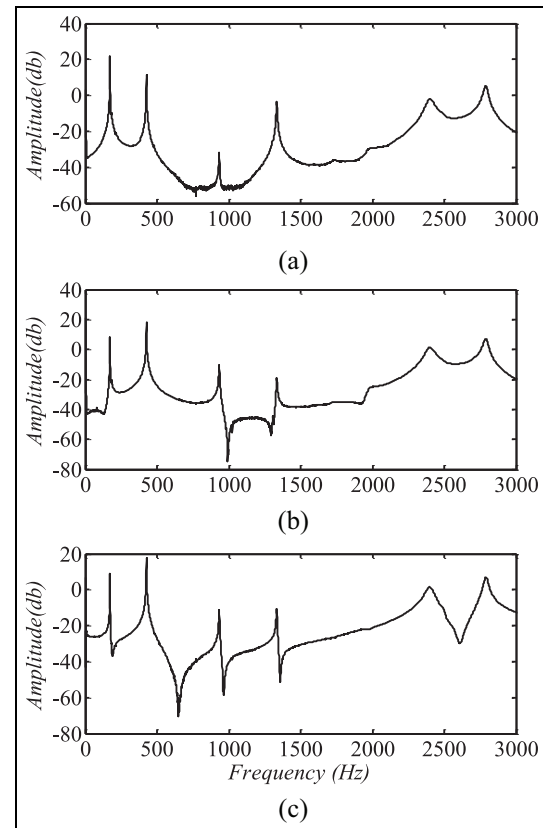


Figure 5. Fast Fourier transform of the acceleration signals: (a) at position x_1 , (b) at position x_2 , (c) at position x_3 .

reproduce the IMF time series. For each IMO, we can extract two time-varying variables: the forcing term of an IMO $F_k^m(t)$ and the dynamic solution of the IMO

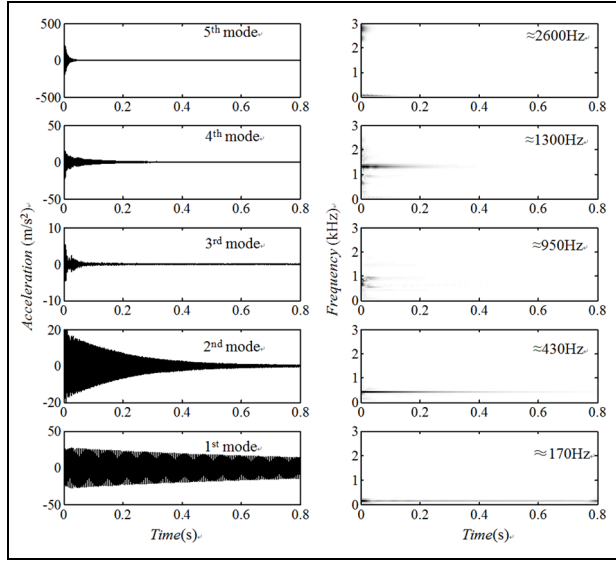


Figure 6. Five dominant IMFs extracted from the acceleration response at position x_1 and the corresponding instantaneous frequencies in wavelet transform spectra.

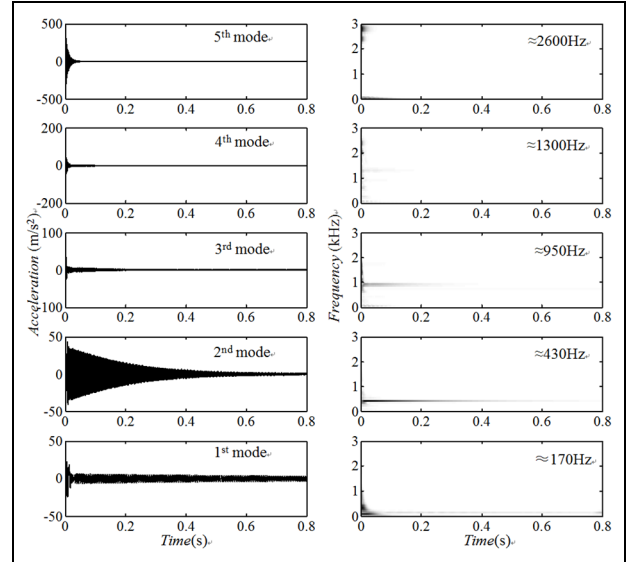


Figure 8. Five dominant IMFs extracted from the acceleration response at position x_3 and the corresponding instantaneous frequencies in wavelet transform spectra.

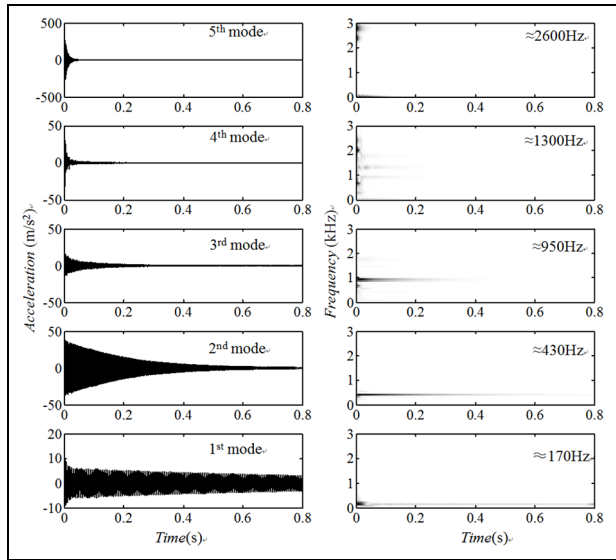


Figure 7. Five dominant IMFs extracted from the acceleration response at position x_2 and the corresponding instantaneous frequencies in wavelet transform spectra.

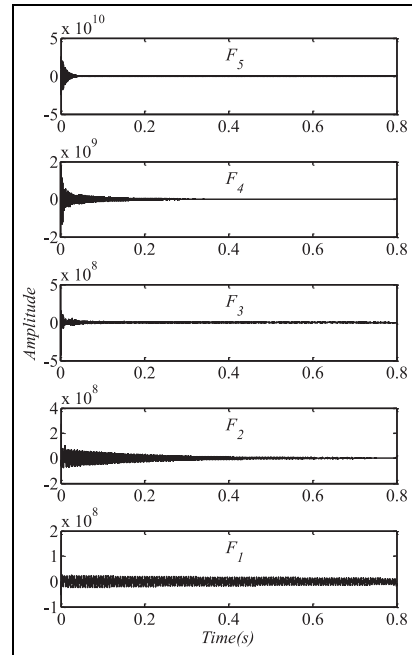


Figure 9. Values of the time-varying coefficient: $F(t)$

$x_k^m(t)$. In this article, these two kinds of time-varying variable are used in equation (17) to calculate damage features for different damage states.

DI using $F_k^m(t)$. The time-varying variables obtained for the case of standard bolt torque (24 Nm) are considered as the reference healthy variables. Figure 11 shows the damage features obtained by using the time variable of

$F_k^m(t)$ at the positions x_1 , x_2 and x_3 . Since the reference healthy condition has 24 Nm torque, for any damaged conditions, the DI value should be less than 1. The results shown in Figure 11 indicate the more severe the damage condition, the lower the DI. It can be found that for a damage condition with torque much lower than 24 Nm, the value of the DI is much lower than 1.

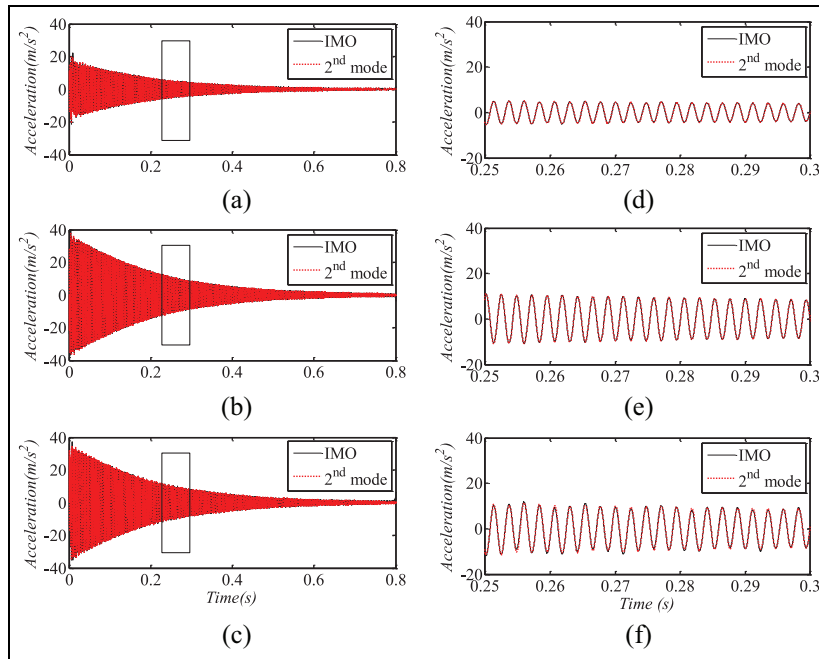


Figure 10. Comparisons of second IMO solutions with the corresponding IMFs (a) at position x_1 , (b) at position x_2 , (c) at position x_3 , (d) the zoom view of result at position x_1 , (e) the zoom view of result at position x_2 , and (f) the zoom view of result at position x_3 .

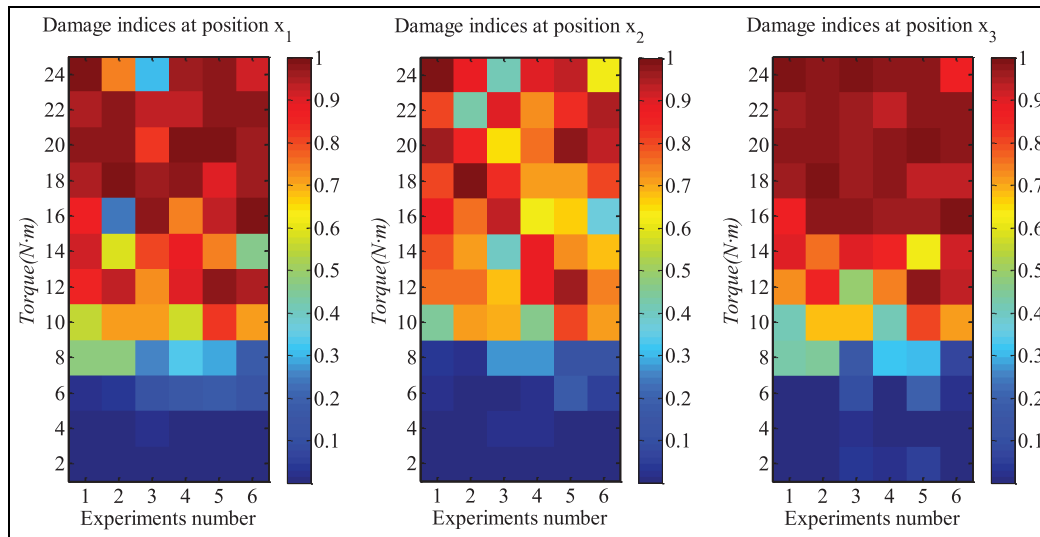


Figure 11. Damage features obtained from three sensor positions.

The color in each figure can distinguish each figure into two parts roughly. The lower part has very low DI and the upper part has high DI. Therefore, it is obvious that the figure can be used to distinguish severe structure damage state. In addition, it can be observed that at different sensor positions, the calculated damage features show different sensitivities. Figure 12 shows the detailed damage feature values for each repeated test and their average values at different sensor

positions. It can be found that as the torque value increase, the proposed damage feature increases, which indicate the proposed damage feature can be used to indicate the change of torque value. A sudden change of the trend at about the torque value 10 Nm is observed. Meanwhile, at each torque value, a large variation of damage feature values can be seen, which indicate the robustness of the damage feature is not good.

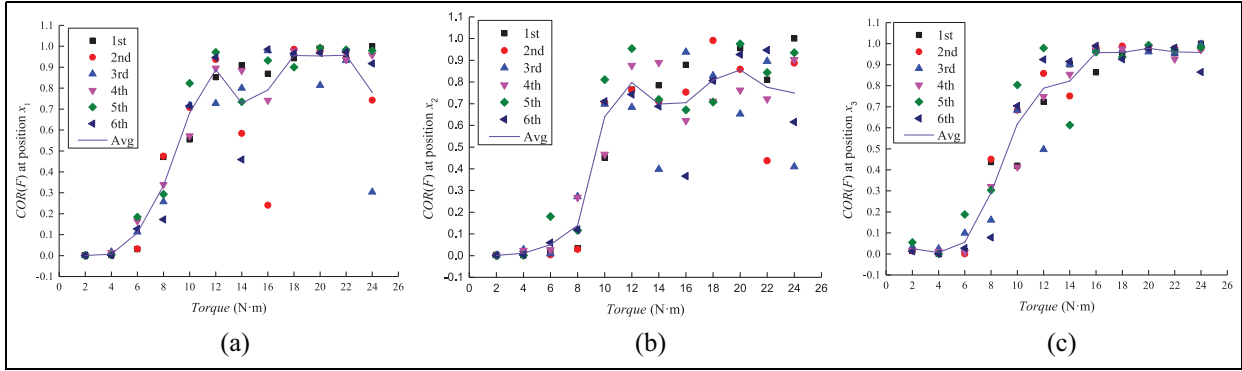


Figure 12. Damage features under different bolt torques: (a) at position x_1 , (b) at position x_2 , (c) at position x_3 .

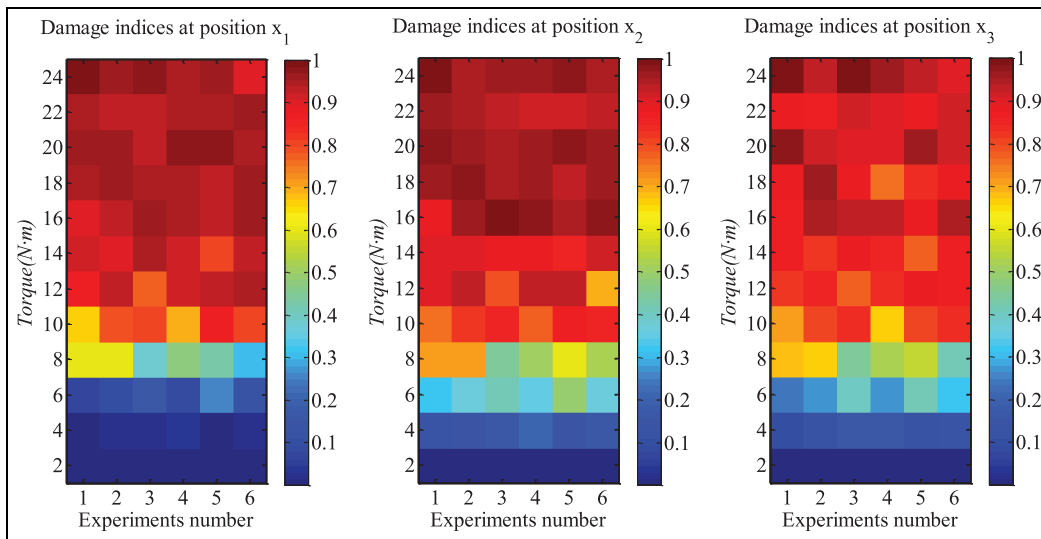


Figure 13. Damage features obtained from three positions.

DI using $x_k^m(t)$. Then, we compute the damage feature by using the IMO dynamic solutions. The time-varying IMO responses obtained for the case of standard bolt torque (24 Nm) are considered as the reference healthy variable. Figure 13 shows the damage features obtained by using the time variable of $x_k^m(t)$ at the positions x_1 , x_2 , and x_3 , respectively. It can be found the same trend relation for the damage features and the bolt torques when compared to Figure 11. However, the variation of damage features improves largely. Figure 14 gives the detailed damage feature values for each repeated test and their average values at different sensor positions. It is clear that the proposed damage feature increases with the increase of the torque values. It means when the bolt is loosened, the proposed damage indicator will decrease. Thus, the proposed damage identification method and damage indicator can be used for bolt loosening detection. Compared to Figure 12, it can be found that the robustness of the damage feature calculated by the IMO dynamic solutions is better. This may

be due to the fact that the dynamic solution includes the effect of IMO stiffness and damping parameters, which causes the IMO dynamic solution to better represent the system dynamics. In addition, the sensitivity of damage feature with bolt torque at different sensor positions is different. It is obvious that the sensitivity of damage feature at the position x_2 and x_3 is better than at the position x_1 . Thus, the sensors installed closer to the joint can give better detection ability.

Conclusions

In this article, the EMD-based NSI method is utilized and extended to solve the problem of identifying bolt loosening in a jointed beam. The EMD method with the techniques of mirror-image signal and masking signal is used to process the recorded dynamic response signals. Based on the EMD, a nonlinear reduced-order model is built to represent the dynamics of the underlying system. A new bolt loosening detection method

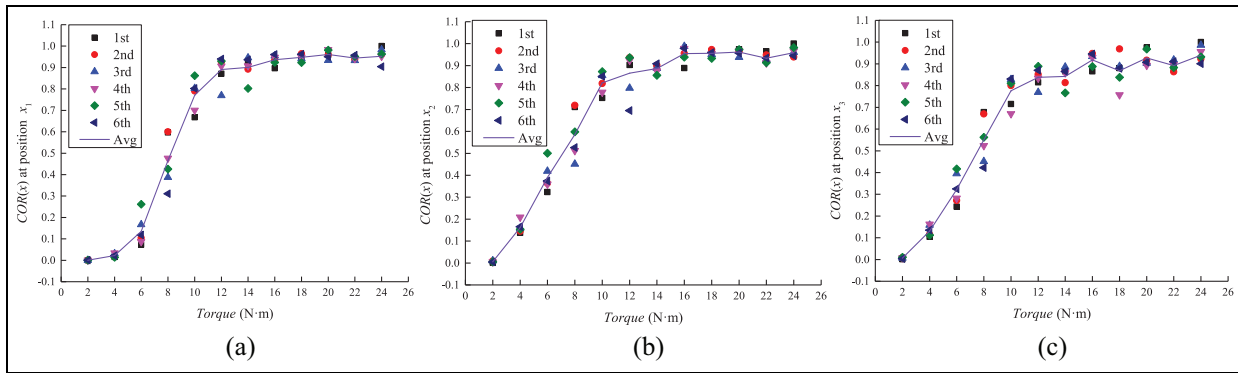


Figure 14. Damage features under different bolt torques: (a) at position x_1 , (b) at position x_2 , (c) at position x_3 .

based on the identified reduced-order model is proposed. A new damage feature to indicate bolt loosening is proposed. Two different time-varying variables from the constructed reduced-order models are used to calculate the proposed damage features.

Experimental works are carried out to validate the proposed loosening detection method. A jointed beam with a central lap joint is considered. The results show that the proposed damage detection can detect bolt loosening effectively, and the proposed damage feature values increase with the increase of bolt torques. The damage feature calculated from the dynamic solution of constructed reduced-order model can give robust and effective indication of bolt loosening. The sensor installed closer to the joint has better sensitivity. This work can be considered as a proof-of-concept study to quantitatively identify bolt torques. By the proposed method, only one sensor is needed to calculate damage feature to indicate bolt torques at a certain location. However, this method can be extended to include more sensors. For example, one potential direction is using a dense array of acceleration sensors and correlation information among those sensors to identify both the bolt loosening locations and bolt torques.

Declaration of conflicting interests

The author(s) declared no potential conflicts of interest with respect to the research, authorship, and/or publication of this article.

Funding

The author(s) disclosed receipt of the following financial support for the research, authorship, and/or publication of this article: This research was funded by China Science Challenge Project of grant number TZ2018007 and China NSAF project of grant number U1530139. The authors would like to thank Professor Mehmet Kurt at Stevens Institute of Technology for the constructive discussions on the NSI method.

ORCID iDs

Chao Xu  <https://orcid.org/0000-0003-3029-1657>

Wei-Dong Zhu  <https://orcid.org/0000-0003-2707-2533>

References

- Peairs DM, Park G and Inman DJ. Practical issues of activating self-repairing bolted joints. *Smart Mater Struct* 2004; 13(6): 1414–1423.
- Doebling SW, Farrar CR and Prime MB. A summary review of vibration-based damage identification methods. *Shock Vib Digest* 1998; 30(2): 91–105.
- Farrar CR and Worden K. An introduction to structural health monitoring. *Philos T R Soc Lond* 2007; 365(1851): 303–315.
- Yang J and Chang FK. Detection of bolt loosening in C–C composite thermal protection panels: I. Diagnostic principle. *Smart Mater Struct* 2006; 15(2): 581–590.
- Amerini F and Meo M. Structural health monitoring of bolted joints using linear and nonlinear acoustic/ultrasound methods. *Struct Health Monit* 2011; 10(6): 659–672.
- Zhang Z, Liu M, Su Z, et al. Quantitative evaluation of residual torque of a loose bolt based on wave energy dissipation and vibro-acoustic modulation: a comparative study. *J Sound Vib* 2016; 383: 156–170.
- Tao W, Shaopeng L, Junhua S, et al. Health monitoring of bolted joints using the time reversal method and piezoelectric transducers. *Smart Mater Struct* 2016; 25(2): 025010.
- Parvasi SM, Ho SCM, Kong Q, et al. Real time bolt preload monitoring using piezoceramic transducers and time reversal technique—a numerical study with experimental verification. *Smart Mater Struct* 2016; 25(8): 085015.
- Doyle D, Zagari A, Arritt B, et al. Damage detection in bolted space structures. *J Intell Mater Syst Struct* 2010; 21(3): 251–264.
- Mascarenas DDL. *Development of an impedance method based wireless sensor node for monitoring of bolted joint preload*. San Diego, CA: University of California, San Diego, 2006.

11. Pavelko I, Pavelko V, Kuznetsov S, et al. Bolt-joint structural health monitoring by the method of electromechanical impedance. *Aircr Eng Aerosp Tech* 2014; 86(3): 207–214.
12. Palacz M and Krawczuk M. Vibration parameters for damage detection in structures. *J Sound Vib* 2002; 249(5): 999–1010.
13. Todd MD, Nichols JM, Nichols CJ, et al. An assessment of modal property effectiveness in detecting bolted joint degradation: theory and experiment. *J Sound Vib* 2004; 275(3): 1113–1126.
14. Nichols JM, Nichols CJ, Todd MD, et al. Use of data-driven phase space models in assessing the strength of a bolted connection in a composite beam. *Smart Mater Struct* 2004; 13(2): 241–250.
15. Caccese V, Mewer R and Vel SS. Detection of bolt load loss in hybrid composite/metal bolted connections. *Eng Struct* 2004; 26(7): 895–906.
16. Milanese A, Marzocca P, Nichols JM, et al. Modeling and detection of joint loosening using output-only broadband vibration data. *Struct Health Monit* 2008; 7(4): 309–328.
17. Huda F, Kajiwara I, Hosoya N, et al. Bolt loosening analysis and diagnosis by non-contact laser excitation vibration tests. *Mech Syst Signal Pr* 2013; 40(2): 589–604.
18. Esmaeel RA and Taheri F. Application of a simple and cost-effective method for detection of bolt self-loosening in single lap joints. *Nondestructive Test Eval* 2013; 28(3): 208–225.
19. Gaul L and Lenz J. Nonlinear dynamics of structures assembled by bolted joints. *Acta Mech* 1997; 125(1): 169–181.
20. Farrar CR, Worden K, Todd MD, et al. *Nonlinear system identification for damage detection*. Los Alamos, NM: Los Alamos National Laboratory, 2007.
21. Crawley EF and Aubert AC. Identification of nonlinear structural elements by force-state mapping. *AIAA J* 1986; 24(1): 155–162.
22. Ma X, Bergman L and Vakakis A. Identification of bolted joints through laser vibrometry. *J Sound Vib* 2001; 246(3): 441–460.
23. Zhang M, Shen Y, Xiao L, et al. Application of subharmonic resonance for the detection of bolted joint loosening. *Nonlinear Dynam* 2017; 88(3): 1643–1653.
24. Roettgen DR and Allen MS. Nonlinear characterization of a bolted, industrial structure using a modal framework. *Mech Syst Signal Pr* 2017; 84: 152–170.
25. Huang NE, Shen Z, Long SR, et al. The empirical mode decomposition and the Hilbert spectrum for nonlinear and non-stationary time series analysis. *P R Soc Lond A Mat* 1998; 454(1971): 903–995.
26. Lee YS, Vakakis AF, McFarland DM, et al. A global-local approach to nonlinear system identification: a review. *Struct Control Health Monit* 2010; 17(7): 742–760.
27. Vakakis AF, Bergman LA, McFarland DM, et al. Current efforts towards a non-linear system identification methodology of broad applicability. *Proc IMechE, Part C: J Mechanical Engineering Science* 2011; 225(11): 2497–2515.
28. Lee YS, Tsakirtzis S, Vakakis AF, et al. Physics-based foundation for empirical mode decomposition. *AIAA J* 2009; 47(12): 2938–2963.
29. Lee YS, Vakakis AF, McFarland DM, et al. Non-linear system identification of the dynamics of aero elastic instability suppression based on targeted energy transfers. *Aeronaut J* 2010; 114(1152): 61–82.
30. Tsakirtzis S, Lee YS, Vakakis AF, et al. Modeling of nonlinear modal interactions in the transient dynamics of an elastic rod with an essentially nonlinear attachment. *Commun Nonlin Sci Numer Simul* 2010; 15(9): 2617–2633.
31. Kurt M, Chen H, Lee YS, et al. Nonlinear system identification of the dynamics of a vibro-impact beam: numerical results. *Archive Appl Mech* 2012; 82: 1461–1479.
32. Chen H, Kurt M, Lee YS, et al. Experimental system identification of the dynamics of a vibro-impact beam with a view towards structural health monitoring and damage detection. *Mech Syst Signal Pr* 2014; 46(1): 91–113.
33. Sadeghi MH and Lotfan S. Identification of non-linear parameter of a cantilever beam model with boundary condition non-linearity in the presence of noise: an NSI- and ANN-based approach. *Acta Mech* 2017; 228(12): 4451–4469.
34. Yu D, Cheng J and Yang Y. Application of EMD method and Hilbert spectrum to the fault diagnosis of roller bearings. *Mech Syst Signal Pr* 2005; 19(2): 259–270.
35. Moore KJ, Kurt M, Eriten M, et al. Elements of a non-linear system identification methodology of broad applicability with application to bolted joints. In: Brake MRW (ed.) *The mechanics of jointed structures*. Cham: Springer, 2018, pp.355–379.
36. Song Y, Hartwigsen CJ, McFarland DM, et al. Simulation of dynamics of beam structures with bolted joints using adjusted Iwan beam elements. *J Sound Vib* 2004; 273(1–2): 249–276.
37. Chao X and Dong W. Experimental investigation of nonlinear interface effects in a jointed beam. *Vibroeng PRO-CEDIA* 2014; 4: 107–112.